FTUV-19-0523.2645, IFIC/19-14, FERMILAB-PUB-19-241-T, NUHEP-TH/19-06

# Looking at the axionic dark sector with ANITA

I. Esteban[1*], J. Lopez-Pavon[2†], I. Martinez-Soler[3,4,5‡], J. Salvado[1§]
[1] *Departament de Fisíca Quàntica i Astrofísica and Institut de Ciències del Cosmos, Universitat de Barcelona, Diagonal 647, E-08028 Barcelona, Spain*
[2] *Instituto de Física Corpuscular, Universidad de Valencia and CSIC, Edificio Institutos Investigación, Catedrático José Beltrán 2, 46980 Spain*
[3] *Theoretical Physics Department, Fermi National Accelerator Laboratory, P.O. Box 500, Batavia IL 60510, USA*
[4] *Department of Physics and Astronomy, Northwestern University, Evanston, IL 60208, USA*
[5] *Colegio de Física Fundamental e Interdisciplinaria de las Américas (COFI), 254 Norzagaray street, San Juan, Puerto Rico 00901.*
(Dated: May 28, 2019)

The ANITA experiment has recently observed two anomalous events emerging from well below the horizon. Even though they are consistent with tau cascades, a high energy Standard Model or Beyond the Standard Model explanation is challenging and in tension with other experiments. We study under which conditions the reflection of generic radio pulses can reproduce these signals. We propose that these pulses can be resonantly produced in the ionosphere via axion-photon conversion. This naturally explains the direction and polarization of the events and avoids other experimental bounds.



*Introduction —*

ANITA (ANtarctic Impulsive Transient Antenna) is a flying radio antenna dedicated to measuring impulsive radio signals in the Antarctica. Its original purpose was the observation of high energy neutrinos via the Askaryan radiation produced by electromagnetic showers in the Antarctic ice [1–3], but a collection of other different impulsive radio signals, such as the ones originated by cosmic ray air showers, can also be triggered. ANITA has a very good angular resolution and is able to discern whether the events are direct or reflected in the ice by measuring the polarization and phase (so-called polarity by the ANITA collaboration) of the radio pulse. Two of the direct cosmic ray events observed in the first and third flights, which seem to be originated well below the horizon (27° and 35° respectively), are particularly intriguing and cannot in principle be interpreted as caused by high energy cosmic-rays [4, 5]. The only standard model (SM) particle that could traverse a large amount of Earth matter (in this case around 6000 and 7000 km) and initiate a particle cascade leading to these events is a very high energy $\mathcal{O}$(EeV) neutrino. However, for these extremely high energies, the neutrino-nucleon cross section leads to a very small survival probability ($\lesssim 10^{-6}$) over the chord length of the events, rendering such interpretation strongly disfavored [6, 7]. Several Beyond the SM (BSM) scenarios have been recently proposed to explain the origin of these events in terms of high energy particles [7–14], but most of them are rather in tension with present data as we briefly describe below.

In order to understand the nature and potential explanation of the ANITA anomalous events we can generically classify the signal origin in two different categories[1]:

- Isotropic, non-transient flux. Unless the corresponding cross section is considerably suppressed, the measurement of two events rather below the horizon ($\sim 30°$) would imply the observation of a much larger amount close to the horizon. Self-consistency of ANITA's data, which does not include any Earth crossing event apart from these two mysterious ones, seems thus to require a cross section much smaller than the typical weak interaction cross section. Even in such a case, the non observation of any similar event by IceCube [15] and Auger [16] makes this possibility unlikely.

- Transient, non-isotropic flux. In this case, ANITA's observed angular event distribution would be consistent. However, generic cosmic ray acceleration mechanisms produce a power-law spectrum, whose low-energy peak would have been detected at IceCube and Auger. Even assuming nothing about the transient energy spectrum, IceCube [17] and Auger [18] have approximately 20 and 30 times more integrated exposure, respectively, than ANITA. Thus, assuming that these transient phenomena occur with an approximately constant rate, the probability of observing two events in ANITA and none in IceCube and Auger is, at most, $9 \times 10^{-5}$.

Therefore, any interpretation of the ANITA anomalous events in terms of incoming SM or BSM high-energy par-

*ivan.esteban@fqa.ub.edu
†jacobo.lopez@uv.es
‡ivan.martinezsoler@northwestern.edu
§jsalvado@icc.ub.edu

[1] We refer the reader to [14] for further details.

ticles seems to be clearly disfavored. As discussed in [7, 14], it would require a combined analysis and even a reinterpretation of the IceCube and Auger results.

Two possible exceptions to this general conclusion are the recently proposed SM explanations in terms of transition radiation [19] and reflection on anomalous sub-surface structures [20]. In both cases, the origin of the anomalous events would be a reflected cosmic ray shower. Unless reflection occurs on a rather tilted surface, this hypothesis is in principle in $2.5\sigma$ tension with the observed polarization angle of the first ANITA anomalous event [4]. Interestingly, both explanations predict particular signatures. On the one hand, transition radiation predicts that events with large elevations will be anomalous, in slight tension with current data. On the other hand, sub-surface structures predict some amount of double events. Therefore, dedicated searches and/or more exposure are required to validate these possibilities.

In this Letter, we propose a novel origin for these intriguing signals. We will show that reflected radio waves emerging from incident angles $\sim 30^\circ$ tend to present the polarization properties of the anomalous ANITA events. A high energy reflected cosmic ray shower, though, cannot in principle generate an initial pulse with the adequate phase (for alternative scenarios see [19, 20]). Instead, we propose that the radio signal is generated via the conversion of an axion-like pulse. For the masses suggested by the data, this transformation happens to be resonant in the Earth ionosphere. This process involves very soft ($\mathcal{O}(\mu\text{eV})$) physics, invisible to IceCube and Auger, that ANITA can potentially test with a dedicated analysis.

*Anomalous ANITA events —*

An atmospheric cosmic ray shower produces polarized radio pulses as the charged particles feel the Lorentz force of the Earth magnetic field $\vec{B}_\oplus$. The radio pulse will be linearly polarized perpendicular to $\vec{B}_\oplus$; since the magnetic field in the Antarctica is mostly vertical, the radio signals are essentially horizontally polarized. Furthermore, since a cosmic ray shower has more electrons than positrons, the phase of the radio pulse is well-determined and it can thus be used to distinguish between direct and reflected signals, as it is done in ANITA.

Indeed, ANITA searches for high energy cosmic ray showers looking for radio signals whose plane of polarization is correlated with the local geomagnetic field (geocorr), i.e., mostly horizontally polarized signals. If the mysterious events have a different origin, this geomagnetic correlation is expected to be accidental. However, a reflected electromagnetic wave generically tends to be horizontally polarized. Thus, in the following we will explore the hypothesis of down going radio waves reflected in the Antarctic ice as the origin for these mysterious events.

Fig. 1 shows the expected angular distribution of reflected geocorr events as a function of their elevation $\varepsilon$. We have assumed an incident isotropic flux, linearly polarized with random polarization angles and a given degree of polarization $P_i$. The observed and incident polarization states are related through the Stokes formalism [21]. We have simulated the ANITA experimental response with a Monte Carlo, where the Stokes parameters are computed adding to the signal Gaussian white noise adjusted to reproduce the observed polarization angle uncertainty [22]. The flux peaks at elevations where light reflects close to the Brewster angle $\theta_B \sim 53^\circ$ (corresponding to $\varepsilon \sim -37^\circ$)[2], defined as the angle at which the reflected signal is polarized exactly in the horizontal direction. The elevations of the observed events, within $1\sigma$, are shown in gray; they are both close to the peak.

In Fig. 1 we also show the expected fluxes associated to other relevant hypotheses for the mysterious events previously considered in the literature. First, a SM tau neutrino flux, in dotted, which strongly peaks at the horizon and is therefore highly disfavored. In dash-dotted, we show the expected distribution associated to a generic BSM high energy particle with a nucleon interaction cross section 10 times weaker than that of the SM neutrino. In both cases we propagate the fluxes with the numerical library $\nu$-SQuIDS [23–25]. As it can be seen, the latter hypothesis partially alleviates the tension in the angular distribution, but tension with IceCube and Auger data remains [14]. Another possibility is that ANITA misidentified reflected events originated by ultra high energy cosmic ray (UHECR) air showers, classifying them instead as direct events. This hypothesis, shown in dashed, is in principle disfavored since it would require polarity misidentification by ANITA, which is excluded at $\sim 4.5\sigma$ [22]. However, alternative scenarios have been recently proposed to support this possibility [19, 20].

According to Fig. 1, our hypothesis of reflected radio waves, linearly polarized in random initial directions, explains the up going direction of the two events. The other alternative scenarios shown in the figure predict more events close to the horizon, and so they could be discriminated from our proposal as ANITA accumulates more exposure.

Another key observable in ANITA, not shown in Fig. 1, is the polarization angle. In Fig. 2 we quantify under which initial conditions our proposed hypothesis is able to reproduce the geocorr signal matching not only the angular distribution, but also the observed polarization angle of the anomalous events. The top panels in Fig. 2 show the reflected (orange) and incident (red) polarization angles for both mysterious events assuming that the

[2] The maximum is not exactly at $\theta_B$ because the Earth magnetic field has a small horizontal component, and therefore ANITA searches for events that are slightly tilted with respect to the horizontal.

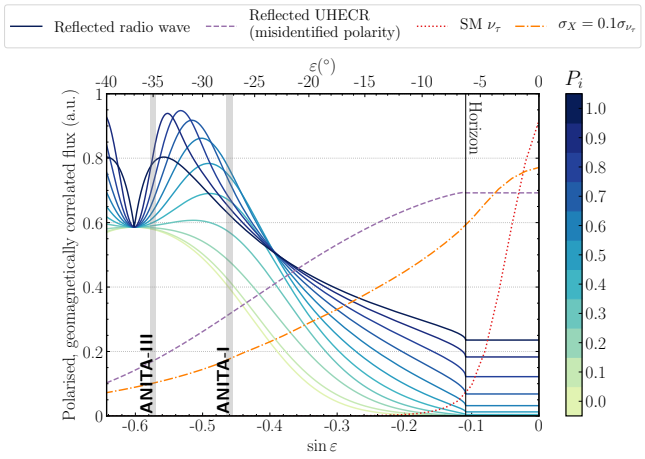


FIG. 1: Expected angular distribution of polarized, geomagnetically correlated events under different hypotheses: an isotropic reflected flux, linearly polarized with an initial degree of polarization labeled by the color and random polarization angles [solid]; reflected UHECRs misidentified as direct [dashed]; a SM $\nu_\tau$ flux [dotted]; and a generic particle with an interaction cross section 10 times smaller than that of the SM $\nu_\tau$. [dot-dashed]. The two ANITA mysterious events are shown in gray. The black line marks the elevation of the horizon, as seen from the ANITA balloon. The elevation range plotted corresponds to ANITA's angular acceptance [26].

signal is fully polarized. For the signal to be identified as an UHECR, the reflected (orange) electric field should be orthogonal to the Earth magnetic field (green), i.e, it should essentially be along the horizontal direction H as it is shown in the figure. The shaded regions correspond to $1\sigma$ uncertainties assuming a $4.6^\circ$ uncertainty in the determination of the polarization direction, and a $2^\circ$ uncertainty in the orientation of the Earth magnetic field [22].

Since both events emerge at elevations close to the Brewster angle $\theta_B$, the vertical (V) component of the reflected electric field becomes quite suppressed. This is the reason why the uncertainty on the incident polarization angle is larger than the uncertainty on the reflected polarization angle. This effect is particularly relevant for the second mysterious event, since it is closer to $\theta_B$ and has a reflected vertical component compatible with 0. The first event, on the other hand, has a non-zero vertical component, which significantly tightens the range of allowed incident polarization angles.

The incident pulse, however, does not need to be fully polarized. To visualize the effect of relaxing this hypothesis, in the middle and bottom panels of Fig. 2 we show the relation among the reflected degree of polarization and polarization angle, $P_r$ and $\psi_r$; and the incident degree of polarization and polarization angle, $P_i$ and $\psi_i$. Since, to our knowledge, the ANITA collaboration has not reported the observed degree of polarization of the events, we have estimated the reflected degree of polarization for which the signal is compatible with being fully polarized within the experimental uncertainty (inferred from our Monte Carlo simulation). The corresponding allowed region is shown in gray in the middle panels.

Comparing the top and bottom panels, we conclude that the range of allowed incident polarization angles increases once we slightly relax the assumption of a fully polarized signal. This is because the unpolarized part of the signal leads to a horizontally polarized component after reflection, which tends to tilt the polarization angle closer to the horizontal, i.e., closer to geocorr. Comparing the ANITA-I and ANITA-III panels, we notice that the level of initial polarization and range of values of the incident polarization angle is less stringent for ANITA-III, as expected since its incident angle is closer to $\theta_B$.

In conclusion, the two mysterious ANITA events have a directionality that can be easily explained via the reflection in the Antarctic ice of an incoming isotropic flux of linearly polarized radio waves in arbitrary directions. Furthermore, the reflection close to the Brewster angle also fits the observed up going cosmic ray-like polarization state.

*Axion-like origin* —

An incoming isotropic flux of linearly polarized radio waves with the required initial conditions to reproduce the observed ANITA signals, though, cannot be easily explained in the SM (see [19, 20] for recent alternative proposals). Below, we will construct a BSM explanation based on the following requirements:

- The source must generate an isotropic flux of impulsive radio signals, spatially isolated and linearly polarized with non-zero vertical component and the correct phase, consistent with Fig. 2.

- Due to the tension with IceCube and Auger data, the production process must not involve high-energy particle cascades.

The first requirement comes from the ANITA triggering system. In particular, the first ANITA flight (ANITA-I) searched for isolated, impulsive, geocorr signals [30]. ANITA-II had a triggering system optimized for Askaryan radiation, whose plane of polarization and spectrum are very different from UHECRs; therefore most of the cosmic ray-like signals were triggered out [31]. Finally, ANITA-III looked for isolated, impulsive events whose signal shape was correlated with a given cosmic ray template [22]. Thus, a source of isolated impulsive signals to pass the ANITA-I and ANITA-III triggers is required.

The second requirement calls for a new physics mechanism able to coherently generate electromagnetic waves. This phenomenon should produce waves with frequencies $\sim \mathcal{O}(1\,\mathrm{GHz})$, i.e., it can be associated with very low energies $\sim \mathcal{O}(10^{-7}\,\mathrm{eV})$. An archetypal BSM example are

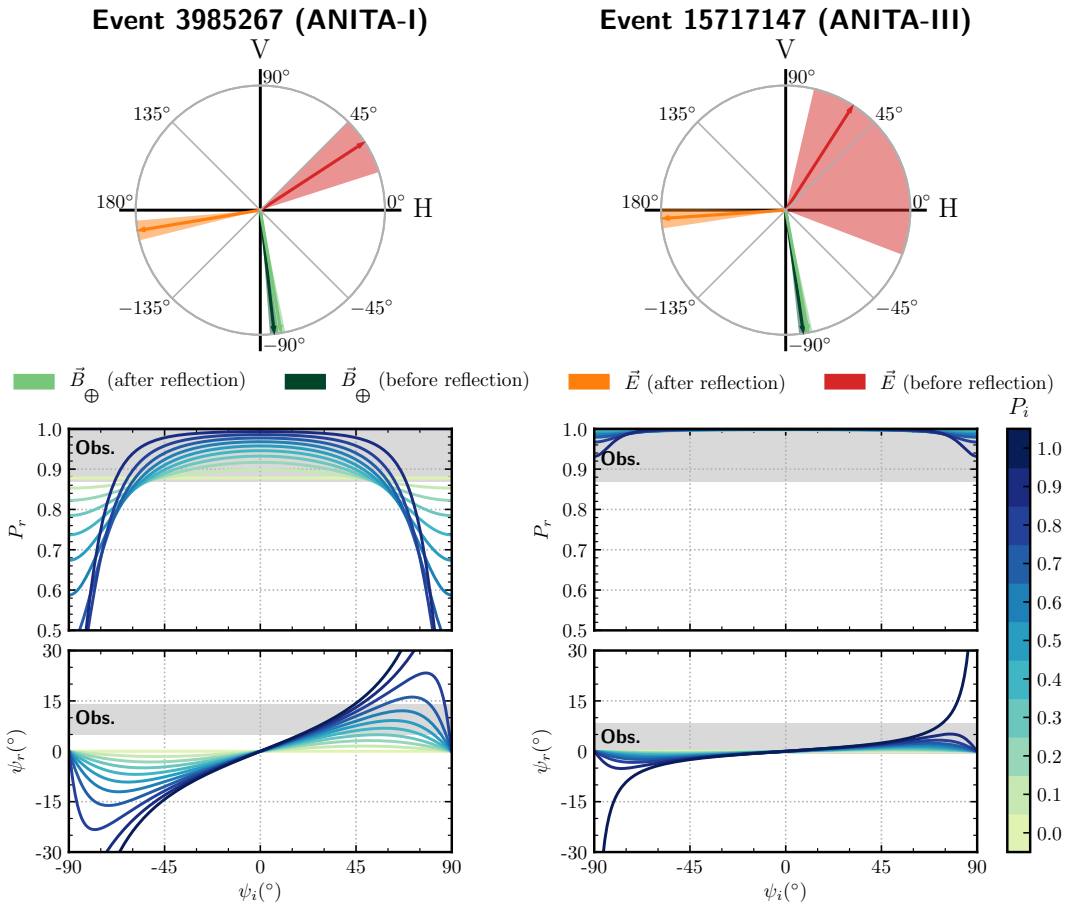


FIG. 2: Top panel: observed (orange) and incident (red) polarization angles. We also show the projection of the Earth magnetic field, extracted from the US/UK World Magnetic Model [27, 28], in the reflected (light green) and incident (dark green) polarization planes. Bottom panel: observed polarization angle $\psi_r$ and degree of polarization $P_r$ as a function of the incident polarization angle $\psi_i$ and degree of polarization $P_i$ (labeled by the color). The allowed $1\sigma$ regions are shown in gray. All angles are measured with respect to the horizontal. We have assumed an index of refraction for the Antarctic surface of $n = 1.35$ [26, 29].

axion-like particles (ALPs), that convert into photons in the presence of an external electromagnetic field.

These particles, first proposed to solve the Strong CP problem [32–34], arise in many models and can naturally be the dark matter in our universe [35–37]. Furthermore, they present self-interactions that produce a very rich phenomenology. In particular, different phenomena, like condensation into a bosonic soliton or instabilities leading to scalar field bursts, may produce impulsive, spatially localized configurations of the scalar field [38–52]. The phenomenology is complex and still under study. In any case, these pulses, with a macroscopic occupation number, may reach us and transform into the electromagnetic pulses observed by ANITA via the interaction with the Earth magnetic field.

The ALPs are generic pseudo-scalar fields $a$ whose interaction with photons is described by the following Lagrangian

$$\mathcal{L} = \frac{1}{2}\left(\partial_\mu a \partial^\mu a - m_a^2 a^2\right) - \frac{1}{4}F_{\mu\nu}F^{\mu\nu} + \frac{1}{4}g_{a\gamma\gamma}aF_{\mu\nu}\tilde{F}^{\mu\nu}\,, \tag{1}$$

with $F_{\mu\nu} = \partial_\mu A_\nu - \partial_\nu A_\mu$ the electromagnetic field strength tensor, and $\tilde{F}^{\mu\nu} = \frac{1}{2}\varepsilon^{\mu\nu\alpha\beta}F_{\alpha\beta}$ its dual. The classical equations of motion for the axion $a$ and electric field $\vec{E}$ in a plasma with free electron density $n_e$ and in presence of an external magnetic field $\vec{B}^\oplus$ are given by [53, 54]

$$\left[\partial_z^2 + \omega^2 + \begin{pmatrix} -\omega_p^2 & -i\omega_p^2\frac{\Omega_z}{\omega} & 0 \\ iw_p^2\frac{\Omega_z}{\omega} & -\omega_p^2 & -g_{a\gamma\gamma}B_y^\oplus\omega^2 \\ 0 & -g_{a\gamma\gamma}B_y^\oplus & -m_a^2 \end{pmatrix}\right]\begin{pmatrix} E_x \\ E_y \\ a \end{pmatrix} = 0\,, \tag{2}$$

where we have assumed waves propagating in the $Z$ direction, a magnetic field in the $YZ$ plane, and we have taken the Fourier transform in time. $\omega_p = \sqrt{\frac{4\pi\alpha}{m_e}n_e}$ is

the plasma frequency, and $\Omega_z = \frac{eB_z^{\oplus}}{m_e}$ is the cyclotron frequency of the plasma that controls Faraday rotation. Note that we have safely neglected $\mathcal{O}\left((eB^{\oplus}/m_e)^2\right)$ terms in the above equations.

When the Faraday rotation effects (the non diagonal terms proportional to $\Omega_z$) are switched off, the solution of these equations gives an electromagnetic wave linearly polarized parallel to the external magnetic field. The terms $\propto \Omega_z$ then lead to the rotation of this polarization in the $YZ$ plane.

*Resonance in the ionosphere —*

Eq. (2) is a system of coupled wave equations with two characteristic frequencies, $\omega^2 - \omega_p^2$ and $\omega^2 - m_a^2$. When both frequencies are equal, axions convert resonantly into photons [53–55].

An incoming axionic pulse would necessarily cross the ionosphere before reaching the Antarctic surface and, depending on the axion mass, undergo a resonant transition. ANITA, together with its low-energy antenna ALFA, is sensitive to frequencies in the range $0.25\,\mathrm{GHz} \lesssim \omega \lesssim 4\,\mathrm{GHz}$. Since the frequency of a wave cannot be smaller than its mass, an axionic interpretation of the mysterious events requires $m_a \lesssim 10^{-7}\,\mathrm{eV}$. These masses happen to be in the range of typical $\omega_p$ values of the Earth ionosphere [56], and thus an incoming axionic pulse with $m_a \lesssim 10^{-7}\,\mathrm{eV}$ would necessarily cross a region where $m_a \sim \omega_p$, resonantly transforming into electromagnetic waves. This phenomenon is analogous to the resonant MSW solar neutrino oscillations [57, 58].

The resonant conversion takes place in a relatively narrow region $\mathcal{O}(10\,\mathrm{km})$. The produced radio pulse will initially be polarized parallel to the Earth magnetic field, with a phase that depends on the axionic wave phase and the sign of the axion-photon coupling $g_{a\gamma\gamma}$. This signal will later traverse the remaining part of the ionosphere, rotating its polarization vector due to the Faraday effect.

Eq. (2) can be approximately solved close to the resonance using the WKB and stationary phase approximations [59]

$$|E|^2 = |a_0|^2 \left(\frac{2 g_{a\gamma\gamma} B_y^{\oplus} \omega^2}{m_a^2}\right)^2 \left[\frac{\pi}{4} \frac{m_a^2/k^2}{\left.\frac{\mathrm{d}\omega_p^2/m_a^2}{k\,\mathrm{d}z}\right|_{\mathrm{res}}}\right], \qquad (3)$$

where $E$ is the electric field after the resonance, $a_0$ is the amplitude of the incoming axion field, $k = \sqrt{\omega^2 - m_a^2}$ is the wave number, $B_y^{\oplus}$ is the Earth magnetic field component in the y-direction, and the derivative is evaluated in the resonance. The term inside the parentheses is the amplitude of the axion to photon conversion in vacuum, while the term inside the square brackets gives the enhancement due to the resonance in the plasma.

In order to numerically solve Eq. (2), we have considered a Chapman-layer ionospheric profile [56, 60]

$$n_e(z) = n_e^{\max} \exp\left\{\frac{1}{\alpha}\left[1 - \frac{\mu - z}{\sigma} - \exp\left(-\frac{\mu - z}{\sigma}\right)\right]\right\}, \qquad (4)$$

$n_e^{\max}$, $\alpha$, $\sigma$ and $\mu$ are phenomenological parameters which control the maximum and shape of the profile, and $n_e^{\max}$ approximately varies between $\sim 10^5\,\mathrm{cm}^{-3}$ and a few times $\sim 10^6\,\mathrm{cm}^{-3}$ [56]. Since the ionosphere profile is not very well known, presenting a considerable uncertainty and temporal fluctuation [56], we have considered two plausible values for the maximum free electron density $n_e^{\max} = 10^5\,\mathrm{cm}^{-3}, 2\cdot 10^6\,\mathrm{cm}^{-3}$ in order to illustrate how the resonant transition takes place. The results for the numerical solution are shown and compared with the analytical approximation, given by Eq. (3), in Figs. 3 and 4.

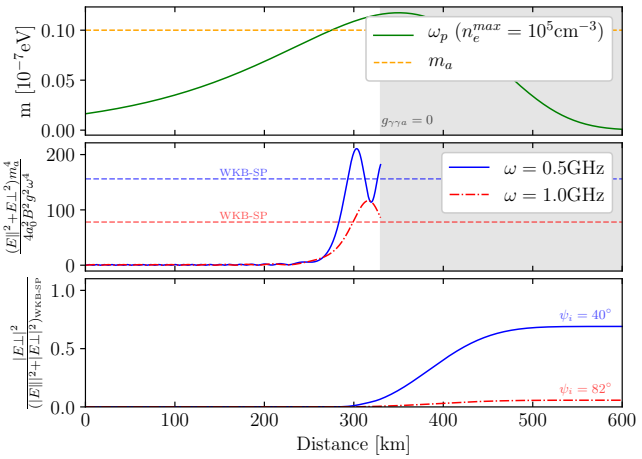


FIG. 3: Top panel: $\omega_p$ profile in the ionosphere, assuming a Chapman layer, along with the axion mass chosen in the simulation. Central panel: electric field squared amplitude, normalized to the vacuum axion-photon conversion squared amplitude. In dashed, we show the result using the analytical approximation given by Eq.(3). In the shaded gray region, we have switched off the axion-photon coupling in order to show only the propagation of the first resonant burst. Bottom panel: squared component of the electric field perpendicular to the Earth magnetic field, generated via Faraday rotation. We have normalized it to the total squared amplitude as given by Eq.(3).

Generically, the axion burst will cross the resonant region twice. In Figs. 3 and 4, we show the resonant conversion taking place at the highest and lowest altitudes respectively. In both figures, the top panel shows the plasma frequency $\omega_p$ as a function of the propagated distance in the ionosphere, together with the axion mass $m_a$ values considered: $10^{-8}\,\mathrm{eV}$ and $4.5\times 10^{-8}\,\mathrm{eV}$ respectively; the resonance takes place when both lines coincide. The central panel shows the total electric field squared amplitude due to resonant axion-photon conversion for different frequencies, normalized to the vacuum

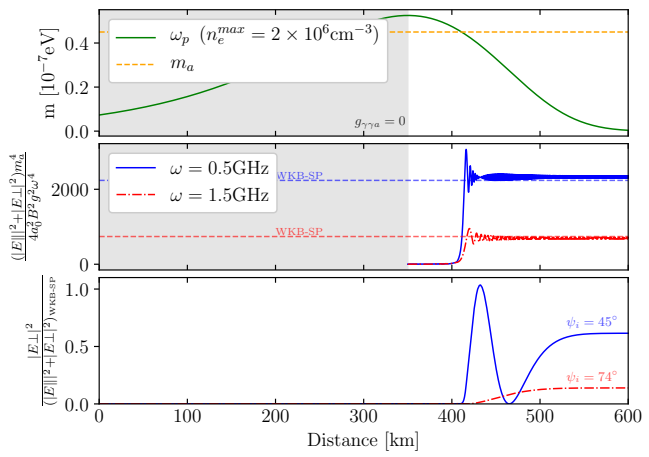


FIG. 4: Same as Fig. 3. Here, we have turned off the interaction in the first resonant region, shown in gray, in order to show only the propagation of the second burst.

squared amplitude. In dashed, we show the approximated solution given by Eq. (3). Finally, the bottom panel shows the squared projection of the electric field in the direction perpendicular to the Earth magnetic field, generated due to Faraday rotation.

The enhancement factor with respect to the vacuum axion-photon transition, observed in Figs. 3 and 4, can be qualitatively understood using Eq. (3). In the ionosphere, $\omega_p$ varies over distances $\mathcal{O}(10\,\mathrm{km})$, much larger than the wavelengths that can be observed by ANITA, $\mathcal{O}(\mathrm{m})$. Therefore, the denominator in Eq. (3) is rather small, leading to an $\mathcal{O}(10^2 - 10^3)$ global enhancement.

The projection of the electric field shown in the bottom panels of Figs. 3 and 4 is directly related to the polarization angle of the radio pulse:

$$\psi_i \approx 6.5^\circ + \arccos\left\{\sqrt{|E_\perp|^2/(|E_\perp|^2 + |E_\parallel|^2)}\right\}, \qquad (5)$$

where $6.5^\circ$ is approximately the slight deviation of the earth magnetic field with respect to the vertical direction V (see Fig. 2). The polarization angle of the pulse when it leaves the ionosphere is indicated in both figures. Notice that in both cases we can fulfill the initial conditions required to reproduce ANITA's anomalous signals, summarized in Fig. 2. In particular, for $\omega = 0.5\,\mathrm{GHz}$ [the solid blue lines in Fig. 3(4)] we obtain an initial polarization angle of $\psi_i \approx 40^\circ\,(45^\circ)$, in agreement with Fig. 2. For $\omega = 1.5\,\mathrm{GHz}$ [dot-dashed red lines] we have, $\psi_i \approx 82^\circ\,(74^\circ)$ in Fig. 3 (4). The latter are consistent with ANITA-III but in disagreement with ANITA-I. This is because in this case the Faraday rotation effect does not generate enough horizontal (essentially orthogonal to $\vec{B}^\oplus$) component of the electric field to reproduce the first event. A different ionospheric profile and/or $m_a$, though, would in general give a different result.

Figs. 3 and 4 are just an example to illustrate how the resonant production mechanism takes place in the ionosphere. In general, since the propagation through the ionosphere partially unpolarizes and decoheres the radio pulse generated during the resonance, there is a trade-off between having enough ionosphere to generate the Faraday rotation required to match the signals (see Fig. 2) and keeping the pulse coherent. These effects are mainly controlled by the density of free electrons $n_e$ in the ionosphere, which can vary in more than one order of magnitude [56]. Therefore, we can distinguish different phenomenological scenarios depending on the value of $n_e^{max}$. For instance, for low values, $n_e^{max} \sim 10^4\mathrm{cm}^{-3}$, the pulse produced in the second resonant region will not undergo Faraday rotation, producing a mostly vertically polarized (parallel to $\vec{B}^\oplus$) signal. This pulse would be triggered out by the ANITA analysis or strongly suppressed due to the reflection close to $\theta_B$. However, the pulse generated during the first resonance would potentially be detectable. For high ionizations, $n_e^{max} \sim 10^6\mathrm{cm}^{-3}$, the first resonantly produced pulse would become incoherent, but the one generated in the second resonance would still be coherent and also experience enough Faraday rotation enough Faraday rotation to pass ANITA's triggers. We have checked, for different configurations, that the resonantly generated pulses can remain coherent enough while undergoing sufficient Faraday rotation. Finally, we would like to remark that the fluctuation in time of the ionosphere leads to different profiles and, thus, pulses experiencing different levels of Faraday rotation can be generated. This means that pulses with diverse polarization directions can leave the inosphere. In other words, the resulting radio waves would potentially mimic the incoming isotropic, linearly polarized flux assumed in Fig.1.

In summary, the ANITA anomalous events could be due to an axionic burst that resonantly converts into photons in the Earth ionosphere. The polarization vector of these photons, initially polarized parallel to the Earth magnetic field, undergoes Faraday rotation during the propagation through the ionosphere. It can therefore match the conditions of the isotropic, linearly polarized flux previously discussed above and shown in Figs. 1 and 2, required to reproduce the signal. Our proposal is schematically summarized in Fig. 5.

*Spectral properties and ALP scenario* —

The characteristics of the observed ANITA events can also be used to extract properties of the ALP burst.

On the one hand, we can infer information about the frequency of the burst. Both anomalous events show a large correlation with a cosmic-ray template, and [5] shows the Amplitude Spectral Density of the ANITA-III anomalous event. We have checked that both spectral requirements can be satisfied within experimental uncertainties using a Gaussian pulse with central frequency $\omega \lesssim 2.5\,\mathrm{GHz}$ and width $\sigma_\omega = 1.5 - 4\,\mathrm{GHz}$.

On the other hand, we can also extract information

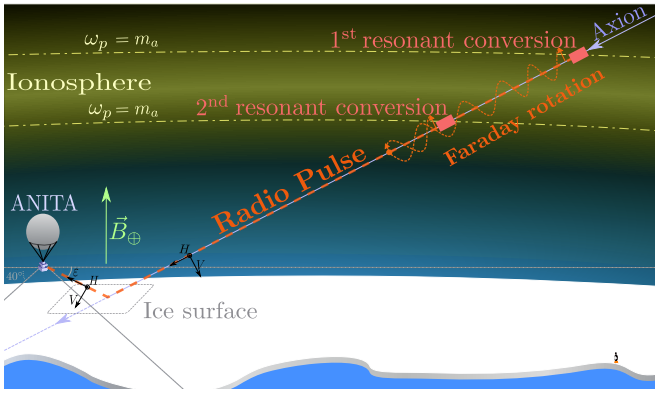


FIG. 5: Sketch of an axion burst arriving to the ionosphere, undergoing resonant conversion, Faraday rotation, and reflecting on the ice surface before reaching ANITA.

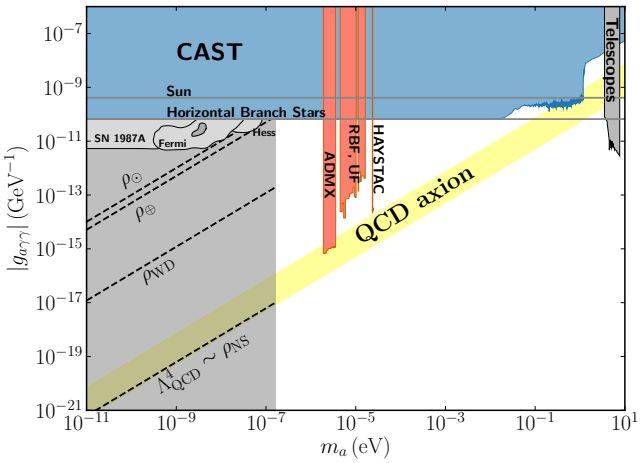


FIG. 6: In gray, estimated axion mass $m_a$ and axion-photon coupling $g_{a\gamma\gamma}$ consistent with the ANITA events for different densities $\rho$ of the incoming axion burst. We plot the result for the Sun and Earth densities $\rho_\odot$ and $\rho_\oplus$, typical densities of a white dwarf $\rho_{\rm WD}$ and neutron star $\rho_{\rm NS} \sim \Lambda_{\rm QCD}^4$, with $\Lambda_{\rm QCD}$ the QCD scale. The minimum observed frequency $\omega \gtrsim 0.25\,{\rm GHz}$ forces $m_a \lesssim 1.6 \cdot 10^{-7}\,{\rm eV}$. We also show current experimental constraints [61, 62].

on the mass and coupling of the ALP. Using Eq. (3), which turns out to be a reasonably good approximation according to Figs. 3 and 4, we can relate the observed electric field amplitude $\sim 1\,{\rm mV/m}$ to the axion mass $m_a$ and coupling $g_{a\gamma\gamma}$, as a function of the amplitude of the axionic field burst. The latter can, in turn, be determined by the energy density of the axionic burst $\rho \sim |a_0|^2\omega^2$. Assuming typical resonance-enhancement factors $\frac{{\rm d}\omega_p^2/m_a^2}{{\rm dz}} \sim 10^{-2}{\rm km}^{-1}$ and a wave frequency $\omega \sim 1.5\,{\rm GHz}$, in Fig. 6 we show an estimation for the values $g_{a\gamma\gamma}$ and $m_a$ consistent with the ANITA data for different energy densities $\rho$ of the incoming axion burst. We have also considered an input for the Earth magnetic field of $B^\oplus \sim 0.45\,G$ and included attenuation due to reflection.

The gray region shows the mass-coupling range compatible with the minimum observed frequency $\omega \sim 0.25\,{\rm GHz}$. The solid lines are labeled with different densities $\rho$ of the incoming axion burst: for densities higher than $\sim 1\,{\rm g/cm}^3$ all present experimental bounds are evaded.

*Conclusions* —

In this work, we have explored the directional and polarization properties of the anomalous ANITA events 3985267 (ANITA-I) and 15717147 (ANITA-III). We have found that the reflection of an isotropic flux, linearly polarized in arbitrary directions, can naturally accommodate both observables. This is mostly due to the triggering of ANITA, that favors horizontally polarized events, together with reflection close to the Brewster angle.

If the process generating these pulses involves very high energies $\sim$ EeV, it would also produce a signal in other cosmic ray observatories like IceCube and Auger, leading to potential tension. Requiring a polarized flux that is not produced via high-energy cascades, we have proposed a generation mechanism based on the axion-photon conversion in the Earth magnetic field of a classical, high occupation number, axion burst.

Interestingly, we have also found that this conversion is dominated by a resonance naturally occurring in the ionosphere for the radio frequencies observed by ANITA. After traversing the remaining part of the ionosphere, the signal will undergo Faraday rotation, providing pulses polarized in different directions that can explain the anomalous events.

This hypothesis can already be tested reanalyzing the data collected by ANITA, including the fourth flight data currently under analysis. If the hypothesis presented in the second section is correct, relaxing the triggering that requires geomagnetically correlated events should reveal events with a non-suppressed vertical component emerging from angles different from $\theta_B$. On the other hand, an axion-like origin generically predicts two events with different polarizations and/or coherence, since the axion burst experiences two resonant transitions into photons along its propagation through the ionosphere. Extra signals could thus be observed by searching for doubled events which may require decreasing the coherence threshold. Finally, the resonant axion-photon conversion in the ionosphere could also be potentially useful for complementary experimental searches.

*Acknowledgments* —

We would like to thank N.P. Plaza and I. Estévez for useful discussions about geoscience and polarimetry. We also thank A. Caputo, P. Coloma, L. Molina Bueno and S. Witte for discussions and careful reading of the manuscript. This work is supported by EU Networks FP10ITN ELUSIVES (H2020-MSCA-ITN-2015-674896) and INVISIBLES-PLUS (H2020-MSCA-RISE-

2015-690575), by the MINECO grant FPA2016-76005-C2-1-P and by the Maria de Maeztu grant MDM-2014-0367 of ICCUB. JLP acknowledges support by the "Generalitat Valenciana" (Spain) through the "plan GenT" program (CIDEGENT/2018/019). Fermilab is operated by the Fermi Research Alliance, LLC under contract No. DE-AC02-07CH11359 with the United States Department of Energy. I.M.S. acknowledge travel support from the Colegio de Fisica Fundamental e Interdisciplinaria de las Americas (COFI). I.E. acknowledges support from the FPU program fellowship FPU15/03697.

[1] G. A. Askar'yan, Sov. Phys. JETP **14**, 441 (1962), [Zh. Eksp. Teor. Fiz.41,616(1961)].
[2] D. Saltzberg, P. Gorham, D. Walz, C. Field, R. Iverson, A. Odian, G. Resch, P. Schoessow, and D. Williams, Phys. Rev. Lett. **86**, 2802 (2001), hep-ex/0011001.
[3] P. W. Gorham et al. (ANITA), Phys. Rev. Lett. **99**, 171101 (2007), hep-ex/0611008.
[4] P. W. Gorham et al. (ANITA), Phys. Rev. Lett. **117**, 071101 (2016), 1603.05218.
[5] P. W. Gorham et al. (ANITA), Phys. Rev. Lett. **121**, 161102 (2018), 1803.05088.
[6] A. Romero-Wolf et al., Phys. Rev. **D99**, 063011 (2019), 1811.07261.
[7] D. B. Fox, S. Sigurdsson, S. Shandera, P. Meszaros, K. Murase, M. Mostafa, and S. Coutu, Submitted to: Phys. Rev. D (2018), 1809.09615.
[8] J. F. Cherry and I. M. Shoemaker, Phys. Rev. **D99**, 063016 (2019), 1802.01611.
[9] L. A. Anchordoqui, V. Barger, J. G. Learned, D. Marfatia, and T. J. Weiler, LHEP **1**, 13 (2018), 1803.11554.
[10] G.-y. Huang, Phys. Rev. **D98**, 043019 (2018), 1804.05362.
[11] J. H. Collins, P. S. Bhupal Dev, and Y. Sui, Phys. Rev. **D99**, 043009 (2019), 1810.08479.
[12] L. Heurtier, Y. Mambrini, and M. Pierre (2019), 1902.04584.
[13] D. Hooper, S. Wegsman, C. Deaconu, and A. Vieregg (2019), 1904.12865.
[14] J. M. Cline, C. Gross, and W. Xue (2019), 1904.13396.
[15] M. G. Aartsen et al. (IceCube), Phys. Rev. **D98**, 062003 (2018), 1807.01820.
[16] A. Aab et al. (Pierre Auger), Phys. Rev. **D91**, 092008 (2015), 1504.05397.
[17] M. G. Aartsen et al. (IceCube), Eur. Phys. J. **C79**, 234 (2019), 1811.07979.
[18] P. Abreu et al. (Pierre Auger), Astrophys. J. **755**, L4 (2012), 1210.3143.
[19] K. D. de Vries and S. Prohira (2019), 1903.08750.
[20] I. M. Shoemaker, A. Kusenko, P. K. Munneke, A. Romero-Wolf, D. M. Schroeder, and M. J. Siegert (2019), 1905.02846.
[21] D. Goldstein, *Polarized Light* (Marcel Dekker, 2003), 2nd ed., ISBN 0-8247-4053-X.
[22] B. J. Rotter, Ph.D. thesis, Hawai'i U. (2017).
[23] C. A. Argelles Delgado, J. Salvado, and C. N. Weaver, Comput. Phys. Commun. **196**, 569 (2015), 1412.3832.
[24] C. A. Argelles Delgado, J. Salvado, and C. N. Weaver, *SQuIDS*, `https://github.com/jsalvado/SQuIDS` (2014).
[25] C. A. Argelles Delgado, J. Salvado, and C. N. Weaver, *Squids*, `https://github.com/arguelles/nuSQuIDS` (2016).
[26] P. W. Gorham et al. (ANITA), Astropart. Phys. **32**, 10 (2009), 0812.1920.
[27] S. McLean, S. Macmillan, S. Maus, V. Lesur, A. Thomson, and D. Dater, Technical Report NESDIS/NGDC-1, NOAA (2004).
[28] S. Maus, S. Macmillan, S. McLean, B. Hamilton, A. Thomson, M. Nair, and C. Rollins, Technical Report NESDIS/NGDC, NOAA (2010).
[29] P. W. Gorham et al., J. Astron. Inst. **06**, 1740002 (2017), 1703.00415.
[30] S. Hoover, Ph.D. thesis, University of California Los Angeles (2010).
[31] M. J. Mottram, Ph.D. thesis, University College London (2012).
[32] R. D. Peccei and H. R. Quinn, Phys. Rev. Lett. **38**, 1440 (1977).
[33] S. Weinberg, Phys. Rev. Lett. **40**, 223 (1978).
[34] F. Wilczek, Phys. Rev. Lett. **40**, 279 (1978).
[35] J. Preskill, M. B. Wise, and F. Wilczek, Phys. Lett. **B120**, 127 (1983).
[36] L. F. Abbott and P. Sikivie, Phys. Lett. **B120**, 133 (1983).
[37] M. Dine and W. Fischler, Phys. Lett. **B120**, 137 (1983).
[38] R. Ruffini and S. Bonazzola, Phys. Rev. **187**, 1767 (1969).
[39] E. W. Kolb and I. I. Tkachev, Phys. Rev. **D49**, 5040 (1994), astro-ph/9311037.
[40] S. Davidson and M. Elmer, JCAP **1312**, 034 (2013), 1307.8024.
[41] P.-H. Chavanis, Phys. Rev. **D84**, 043531 (2011), 1103.2050.
[42] M. P. Hertzberg, JCAP **1611**, 037 (2016), 1609.01342.
[43] E. Braaten, A. Mohapatra, and H. Zhang, Phys. Rev. Lett. **117**, 121801 (2016), 1512.00108.
[44] J. Eby, P. Suranyi, and L. C. R. Wijewardhana, Mod. Phys. Lett. **A31**, 1650090 (2016), 1512.01709.
[45] J. Eby, M. Leembruggen, P. Suranyi, and L. C. R. Wijewardhana, JHEP **12**, 066 (2016), 1608.06911.
[46] D. G. Levkov, A. G. Panin, and I. I. Tkachev, Phys. Rev. Lett. **118**, 011301 (2017), 1609.03611.
[47] P.-H. Chavanis, Phys. Rev. **D98**, 023009 (2018), 1710.06268.
[48] L. Visinelli, S. Baum, J. Redondo, K. Freese, and F. Wilczek, Phys. Lett. **B777**, 64 (2018), 1710.08910.
[49] P.-H. Chavanis (2018), 1810.08948.
[50] E. Braaten and H. Zhang (2018), 1810.11473.
[51] M. A. Amin and P. Mocz (2019), 1902.07261.
[52] J. Eby, M. Leembruggen, L. Street, P. Suranyi, and L. C. R. Wijewardhana (2019), 1905.00981.
[53] G. Raffelt and L. Stodolsky, Phys. Rev. **D37**, 1237 (1988).
[54] P. Sikivie, Phys. Rev. Lett. **51**, 1415 (1983).
[55] M. Yoshimura, Phys. Rev. **D37**, 2039 (1988).
[56] M. Kelley, *The Earth's Ionosphere: Plasma Physics and Electrodynamics* (Academic Press, 2009), 2nd ed., ISBN 9780120884254.
[57] S. P. Mikheyev and A. Yu. Smirnov, Sov. J. Nucl. Phys. **42**, 913 (1985).
[58] L. Wolfenstein, Phys. Rev. **D17**, 2369 (1978).

[59] A. Hook, Y. Kahn, B. R. Safdi, and Z. Sun, Phys. Rev. Lett. **121**, 241102 (2018), 1804.03145.
[60] S. Chapman, Proceedings of the Physical Society **43**, 26 (1931).
[61] M. Tanabashi et al. (Particle Data Group), Phys. Rev. **D98**, 030001 (2018).
[62] L. Di Luzio, F. Mescia, and E. Nardi, Phys. Rev. Lett. **118**, 031801 (2017), 1610.07593.